FAIR Beam Instrumentation
Design Considerations for Resonant Transformers

A. Reiter, H. Reeg, M. Witthaus
GSI Beam Instrumentation Department

June 19, 2018

Contents

1 Introduction

This short monograph describes boundary conditions for the design and layout of resonant transformer that will be installed in the FAIR facility. Basic equations for estimates are taken from references [1] and [2].

2 General Considerations

A few main boundary condition need to be respected in the RT design which are grouped into categories of geometry, measurement and beam parameters.

2.1 Detector geometry

1. Cost: The total cost of a ring core depends on its total volume (old estimate ∼1 US dollar/cm^3) and, for segmented cores, the complexity of the machining processes involved. A simple-minded optimisation, see appendix A, leads to the requirement of a preferably small outer core radius.

2. HEBT RT: The inner diameter of the ferrite core must exceed the outer diameter of a DN 150 CF flange (outer diameter 203 mm or 8 inch) in order to fit over the ceramic vacuum gap. Note that this means the ferrite core after the windings have been added.

3. The maximum outer dimension for a monolithic core is 260 mm (as stated by A. Patel, National Magnetics Group, Inc. (NMG), in an email on 2nd May 2018). There is no general limit for the core dimension in beam direction.

4. For outer dimensions greater than 260 mm the ferrite core must be segmented. The expected size of a single gap is g = 50 µm. The effective permeability of the ferrite core is reduced according to:

$$\mu_{eff} = \frac{\mu_r}{(1 + \mu_r \cdot Ng/l)} \tag{1}$$

   where μ_r is the realtive permeability of the ferrite material, g the single gap size, N the number of gaps, and l the magnetic length (∼ circumference) of the core.

5. pBar Separator: For the large-aperture RT (>400 mm inner diameter), a ferrite core with 8 segments has been proposed by NMG. The shape may be toroidal or octagonal. The toroid would be ground from the unmachined octagonal blank. For the LA-RT the octagon, better a hexagon, is suitable.

2.2 Measurement goals

1. The calibration pulser of the RT detectors aims for 1 % accuracy.

2. RT amplifier and data acquisition hardware aim for a charge resolution of 1 %.

3. The maximum repetition rate is given by the damping of the oscillation. For typical RTs the signal has decayed within a few ms, a much shorter time compared to the synchrotron cycle times.

4. We define an empirical upper limit for the oscillation frequency of 30 kHz by experience as all existing RTs at GSI operate below this frequency. The skin depth (µm) at a few frequencies is given for reference: 20 kHz/460 ; 30 kHz/375 ; 50 kHz/290 ; 100 kHz/205. Further, this limits core losses that increase strongly at higher frequencies.

We therefore set a threshold of 0.5 % in our calculations when integration error and batch detection are analysed in section 3.

2.3 Beam parameters

Most parameters for the RTs are defined by the design beams of protons and U^{+28} from reference [3]. The maximum extraction rate for standard beam production cycles is below 3 Hz.

1. pBar production:

   - SIS18
     - Structure: single 50 ns (full width) pulse
     - Kinetic energy: E = 4 GeV
     - Beam charge: 6.25x10^{12} protons or 1 µC
     - Mean beam current: 20 A
     - Maximum peak current: 40 A for triangular pulse shape
   - SIS100
     - Structure: single 50 ns (full width) pulse (shortest expected pulse length)
     - Kinetic energy: E = 29 GeV
     - Beam charge: 2.5x10^{13} protons or 4 µC (maximum expected total charge)
     - Mean beam current: 80 A
     - Maximum peak current: 160 A for triangular pulse shape

2. NUSTAR: SIS18 - (SIS100) - S-FRS:

   - SIS18:
     - Structure: one batch of two U^{+28} bunches
     - Kinetic energy: E = 200 MeV/u
     - Beam charge: 1.25x10^{11} or 0.5 µC
     - Revolution frequency: 0.45 MHz (large bunch separation)
   - SIS100:

– Structure: see Fig. 1 for injection
– Bunch offset: $3/4 \cdot \tau_r$/(no. of bunches - 1) between centres of two bunches
– Kinetic energy: E = 400 – 1500 MeV/u
– slow extraction ~2 s to S-FRS
  fast extraction 5x10^{11} U^{+28} or 2.24 µC to storage ring

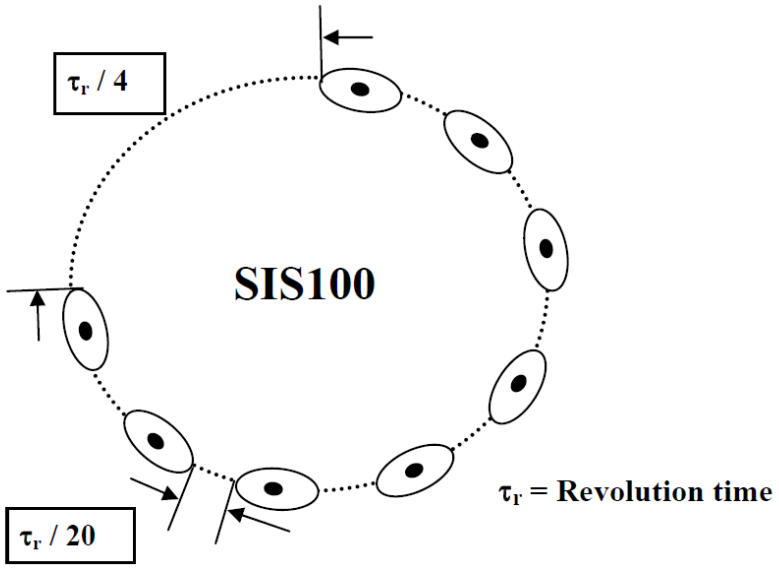

Figure 1: SIS100 bunch filling pattern, taken from TDR SIS100, Fig. 2.8.10.3. With a cirumference of 5 times that of SIS18, one quarter of SIS100 remains empty for an operation with h=10 when 4x2 bunches are injected from SIS18. The minimum bunch distance is $\tau/20$, assuming a bunch length of 50 % of the bunch distance.

While the pBar production chain yields the highes bunch charges of about 4 µC, the NUSTAR production chain imposes an upper limit of the length of a bunch train (or batch) of $\Delta t \sim 2$ µs.
Extraction of batches from SIS100 at low revolution frequencies (small energies) is not part of the standard operation, but may be performed during initial machine commissioning, regular setup or for other purposes. For U^{+28} beams revolution times and bunch offsets are given in Table 1 as function of magnetic rigidity and kinetic energy. See sections 3.2 and 3.3. For high intensity primary beams, the magnetic flux B induced in a small ferrite core may extend over a range in which the permeability is not a constant function any more. The permeability of the material CMD 5005 then tends to increase. This would lead to variations of the angular frequency until resistive losses have reduced the magnetic flux values. See section 3.4. The large-area RTs that will be installed in secondary beam transport lines will not experience the fore-mentioned problems as only one single pulse of moderate to rather low charge content must be detected. This detector must be designed with a high sensitivity.

Table 1: Revolution time in SIS100 for U^{+28}

Mag. rigidity (Tm)	Energy (MeV/u)	Rev. period (ns)	Offset (ns)
12	91	8840	947
18	196	6390	685
40	759	4353	466
60	1380	3960	424
90	2376	3780	404
100	2716	3753	402
v=c	—	3640	390

3 Theoretical Detector Response

The LRC circuit equivalent of a resonant transformer has been described in [4]. To a square pulse of length T the RT responds with a damped oscillation with decay time constant λ and angular frequency ω_0. The total inductance $L_S = n^2 \cdot L_0$ is given by the number of windings n and the inductance factor L_0, the inductance for a single winding (also referred to as A_L). The RT output signal is a composition of two damped oscillation shifted by pulse length T:

$$\lambda[Hz] = \frac{R[\Omega]}{2 \cdot L_S[H]} \quad (1\ \mathrm{H} = 1\ \mathrm{Vs/A} = \Omega\ \mathrm{s}) \tag{2}$$

$$\omega_0[Hz] = \sqrt{\frac{1}{L_S[H] \cdot C[F]} - \lambda[Hz]^2} \tag{3}$$

$$V_C(t)[V] = \frac{-I_B[A]}{n\,\omega_0[Hz]\,C[F]} \cdot e^{-\lambda t} \left[sin(\omega_0 \cdot t) - e^{\lambda \cdot T} sin\left(\omega_0 \cdot (t-T)_{t \geq T}\right) \right] \tag{4}$$

$$\approx \frac{-I_B[A] \cdot T[s]}{n\,C[F]} \cdot e^{-\lambda t}\, cos(\omega_0 t) \quad \text{for T<<1} \tag{5}$$

$$= \frac{-Q[As]}{n\,C[F]} \cdot e^{-\lambda t}\, cos(\omega_0 t) \tag{6}$$

We stress that the last equation is valid for short pulses. The amplitude loss or "integration error", for longer pulses is discussed in setion 3.2. Extensive details on RT construction and response can be found in the diploma thesis by R. Steiner [5]. Since we talk exclusively about the capacitor voltage, the subscript C will be dropped in the remainder of the document.

3.1 Detector sensitivity and maximum voltage

3.1.1 Sensitivity

The RT sensitivity can be estimated according to Equ. 6. The maximum voltage $V_{max} = V(t=0)$ is given by:

$$V_{max}(Q, n, C) = \frac{Q[As]}{n\,C[F]} \tag{7}$$

We define the sensitivity S as the maximum voltage $V_M(Q_{ref})$ for a reference charge of 1x10^8 elementary charges or Q_{ref} =16 pC. It represents the minimum charge that the RT must be able to measure in pBar Separator or HEBT. Now, the voltage is a function of the two "free" RT parameters winding number n and capacitance C (as L_0 is fixed by the ferrite core):

- HEBT prototype with C=2.2 nF and n=150: S∼50 µV
- GSI RT GHTPDT1C with C=0.35 nF and n=100: S∼450 µV

The factor 10 between the two sensitivity values is a result of the different maximum charge values that need to be detected. See section 3.1.2.

The RMS noise of a capacitor is given by $V_{RMS} = \sqrt{\frac{kT}{C}}$ with k the Boltzmann constant and T the temperature. For the 2 nF capacitor we have $V_{RMS} \sim 1.5$ µV. Therefore, the RT amplifier must be able to detect signals in the range of about 10−20 µV, if we hope to detect charges above 5 pC.

3.1.2 Maximum voltage

The sensitivity must be matched to the maximum beam charge to avoid excessive capacitor voltages. If we consider the primary proton beam for pBar production and include a safety factor of 2.5, the maximum charge $Q_{max}(HEBT)$=10 µQ. For an assumed maximum voltage of 50 V, the lower limit of the product $(n \cdot C)$ is defined as:

$$(n \cdot C)_{HEBT} > 2 \cdot 10^{-7} \tag{8}$$

Therefore, the maximum sensitivity for the HEBT RT is 80 µV. The full scale range of the HEBT prototype with S=50 µV corresponds to a voltage V_{max}=30 Volt, while for nominal beam intensity of 4 µC we have $V_{max} \sim 12$ V.

For the maximum charge in the pBar separator we assume $Q_{max}(pBar) = 1\text{x}10^{11}$ π^- =16 nC. In this case, the lower limit for the parameter combination (n, C) is set by the maximum acceptable oscillation frequency and other factors like position independence (minimum number of windings n).

3.2 Integration error and bunch length

If the pulse length T is not negligible, the response to the square pulse is composed of two oscillations with time offset T (see Equ. 4). These can be approximated by one mean oscillation that refers to the bunch centre at $T/2$. The result is a modification of equation 6 with substitution $t \rightarrow (t - T/2)$ and a new multiplicative term, called integration error, that describes the lost amplitude in the signal:

$$V_C(t)[V] = \frac{-Q[As]}{n\,C[F]} \cdot \left(1 - \frac{(\omega_0 T)^2}{24}\right) \cdot e^{-\lambda(t-T/2)}\, cos(\omega_0(t - T/2)) \tag{9}$$

If the amplitude loss is required to be below 0.5%, the maximum pulse length T_{max} is given by:

$$T_{max}(\nu) \leq \frac{\sqrt{24 \cdot 0.005}}{2\pi\nu} = \frac{0.05513}{\nu} \tag{10}$$

This yields $T_{max} = 2756/1838$ ns for $\nu = 20/30$ kHz oscillation frequency, respectively. Single bunches are expected to be much shorter. Hence, the integration error can be safely disregarded even for an integration error of 0.25%.

3.3 Batch detection

The detection of more than one bunch, i.e. batch detection, may also introduce a loss of signal amplitude ("ballistic deficit"), if the offset between bunches becomes too large. In an extreme case the separation is so large that the previous RT response has decayed (no overlap), and all following pulse information would be lost.
We model the output voltage for batch detection analytically as the sum of single responses (Equ. 9), shifted in time by a fixed offset T_O ($t \rightarrow t - T_0$) between successive bunches, to bunches of identical charge. Figure 2 illustrates how the resulting response (black trace) to eight bunches with 500 ns offset between each bunch (blue traces) is shifted with respect to the response to a single bunch carrying the same total charge (red trace). Further, the detected signal amplitude is 1% smaller compared to the response of a single short bunch.

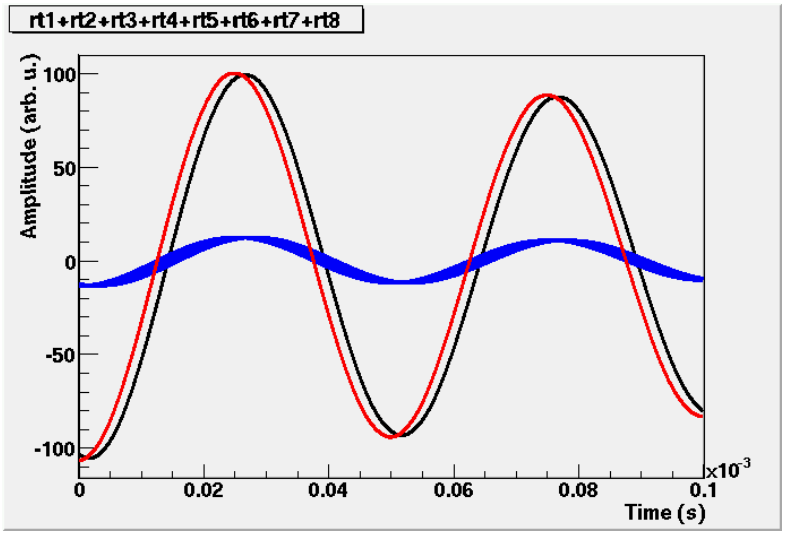

Figure 2: Calculated responses to eight bunches with 500 ns offset (blue), detector response to the batch (black trace), and response to a single pulse (red trace).

The ratios of the maxima for the single bunch responses (for the total charge) and the maxima of the batch responses for 2, 4 or 8 bunches are reported in Tab. 3.3 for oscillation frequencies of 20 kHz and 30 kHz. The calculations were carried out for offsets ranging from 200 ns to 1500 ns. Increasing the bunch length T from 50 ns to 500 ns did not change the results. For 20 kHz oscillation frequency the limit of 0.5% amplitude loss is reached at >1500 ns/750 ns/∼330 ns for two/four/eight bunches, respectively. For 30 kHz oscillation frequency the limit is reached at 1000 ns/500 ns/∼220 ns, respectively.

For the extraction of eight bunches from SIS100 it is obvious from Table 1 that the offsets will be of the order of 500 ns, and hence an amplitude loss of the order of 1% or more must be expected, depending on the oscillation frequency. However, this type of operation is not planned for the reference beam production chains of FAIR.

Finally, we note that the integration error approximates the amplitude loss, if the

Table 2: Signal ratio of single bunch response to model response (sum of single responses for harmonic numbers h = 2, 4, 8) as function of offset between two successive bunches. The ratios were calculated from the maximum values of both functions, assuming two oscillation frequencies of 20 kHz and 30 kHz.

20 kHz oscillation frequency				
T_O (ns)	ratio(h=2)	ratio(h=4)	ratio(h=8)	Comment
200	1	1.0004	1.0026	
300	1.0002	1.0009	1.0037	
400	1.0003	1.0016	1.0067	
500	1.0005	1.0025	1.010	
750	1.0011	1.0053	1.023	
1000	1.0019	1.0094	1.040	
1500	1.0042	1.0214	1.094	
30 kHz oscillation frequency				
T_O (ns)	ratio(h=2)	ratio(h=4)	ratio(h=8)	Comment
200	1.0001	1.0009	1.0037	
300	1.0004	1.0020	1.0084	
400	1.0007	1.0035	1.0151	
500	1.0011	1.0055	1.0237	
750	1.0025	1.0126	1.0545	
1000	1.0045	1.0226	1.1000	
1500	1.0101	1.0519	1.2458	

total pulse length is set to $T_{tot} = (h-1)T_O + 1/2 \cdot T_O$. The last term adds the bunch length to the mean separation between first and last bunch (see Fig. 1). The approximation is consistent with the model calculation to within ∼30 %, especially for the higher harmonic numbers h =4 and 8, when the longer pulse train starts to emulate a continuous distribution.

3.4 Maximum core flux density

The maximum magnetic flux B_{max} induced in the ferrite ring core can be estimated from the maximum current through the coil (see ref. [5], pages 17 and 18). This current is a function of the maximum change in the capacitor voltage:

$$I_{max} = C \cdot \left(\frac{dU}{dt}\right)_{max} \approx C \cdot U_{max} \cdot \omega_0 = \frac{Q}{n} \cdot \omega_0 \tag{11}$$

This current flows through the coil and acts n times on the ferrite:

$$I_{max}(n) = n \cdot I_{max} = Q \cdot \omega_0 \tag{12}$$

We consider the primary proton beam for pBar production, carrying a charge Q=4 µC, for C=2 nF, n=150 and oscillation frequency ν=20 kHz. Inserting into Equ. 11 the maximum voltage $V_C(max) = Q/nC$ =13.3 V leads to a current I_{max} = 3.4 mA that flows from the capacitor. The total current that acts on the ferrite $I_{max}(n) = n \cdot I_{max} = 0.5$ A for all n=150 windings. The same result is obtained directly from Equ. 12.

The magnetic field H_{max} in a ferrite of radius r generated by this current is

$$H_{max} = \frac{I_{max}(n)}{2\pi \cdot r} = 0.8\,\mathrm{A/m} = 0.01\,\mathrm{Oe} \tag{13}$$

Assuming a permeability µ=2000, the magnetic flux B_{max} ∼2 mT or 20 Gauss. At this value we can deduce from available data sheets [6] a permeability change for the CMD 5005 material below 10% and a change in angular frequency ω_0 below 5%.

3.5 Effective quality factor

For the GSI RTs and the FAIR protoype RT, the observed damping factor λ is much larger than the theoretical value $\lambda = R/(2L_S)$ which neglects additional resistive losses, if only the winding resistance is included. Estimates of the effective coil resistance R_e are difficult as they must include ferrite core losses.
At this point the definition of the effective quality factor Q_e is helpful in order to assure that a sufficient number of oscillations is acquired and available for charge analysis:

$$Q_e = \frac{\omega_0 \cdot L_S}{R_e} \tag{14}$$

As example we consider an RT with 20 kHz oscillation frequency. If we require an observation interval of 20 oscillation periods $T_{20} = 20 \cdot T = 1$ ms and a remaining

amplitude of 5% ($V(T_{20}) = 0.05 \cdot V(t = 0)$), this leads to an upper limit $\lambda < 3000$ 1/s. Rewriting Q_e, we obtain:

$$Q_e = \frac{\omega_0 \cdot L_S}{R_e} = \frac{\omega_0}{2\lambda} = \frac{\pi\nu}{\lambda} \approx 20 \tag{15}$$

Quality factors of ferrite materials are readily available from data sheets [6], often however not at the rather low frequencies considered here. CMD 5005 reaches a value of Q_e =22.5 at 50 kHz, and the quality factor should continue to increase towards lower frequencies.

3.6 Effective permeability

The effective permeability for segmented ferrite cores is approximately given by:

$$\mu_{eff} = \frac{\mu_r}{(1 + \mu_r \cdot Ng/l)} \tag{16}$$

where μ_r is the realtive permeability of the ferrit material, g the single gap size, N the number of gaps, and l the magnetic length ($\sim$ circumference) of the core. The total gap size must be much smaller than the magnetic length l: $N \cdot g << l$.
For the pBar Separator we compare different geometries of square, hexagon, octagon and toroid for an inner radius of 210 mm (inner aperture=420 mm) and 40 mm segment thickness (hence 230 mm centre radius for a toroid).

Table 3: Comparison of effective permeability for different geometries. The assumed inner radius is 210 mm and the permeability μ_r=2000.

Parameter	Unit	Square	Hexagon	Octagon	Toroid
no. of segments		4	6	8	4 / 8
gap size g	µm	50			
inner aperture	mm	210			
segment length a	mm	460	265	191	361 / 181
circumference	mm	1840	1590	1528	1445
mag. length l	mm	1840	1590	1528	1445
effective permeability		1643	1451	1311	1566 / 1287

For polygons the total air gap size increases, while the magnetic lengths l drops. Both effects decrease the effective permeability. From square to hexagonal shape the permeability drops by roughly 10 %, and again by a similar value from hexagonal to octagonal shape.
In total, the hexagon seems to be the best choice or compromise with respect to number of segments (air gaps), total magnetic length or circumference (which influences the minimum number of windings), outer diameter and achievable effective permeability.

4 Selection of RT parameters

4.1 Selection approach

In order to investigate an "optimum" choice of RT parameters, we rewrite the sensitivity S for short pulses, perhaps in a rather unusual form, as function of angular frequency ω_0, capacitance C, and inductance L_0 using Equ. 3 (where we have disregarded the second term):

$$S = \frac{Q}{nC} = Q\left(\frac{\omega_0}{\sqrt{C}}\right)\sqrt{L_0} \tag{17}$$

This suggests the following procedure, if the sensitivity is to be optimised for a given maximum angular frequency ω_0 that has been defined for the application:

- Maximise L_0 (which implicitly helps to keep ω_0 small): $L_0 = \mu_0 \cdot \mu_{eff}(A/l)$ with A the ring core cross section and l the magnetic path length (∼circumference of ring core). Remember to keep the total volume V small, see Equ. 22.

- Select the capacitance C: The ratio $(\omega_0/\sqrt{C})$ increases for small values of C. High intensity beams may pose a lower limit to the capacitor value to avoid excessive voltages.

- Calculate number of windings n: Respect the maximum value $\omega_0 \propto 1/n$ by appropriate (as small as possible) choice of n.
  Note that an excessive value can introduce inductive leakage or other parasitic oscillations, and reduces the sensitivity S.

Note that for the HEBT application the high beam intensity imposes an upper limit on the maximum sensitivity S. Then, the requirement on the inductance factors can be relaxed. However, if the RT amplifier operates with more than one capacitor across different gains in order to boost the sensitivity for smaller charge measurements, the increase in oscillation frequency should be kept in mind.

4.2 RT for HEBT

Different options for the HEBT are compared in table 4. For the HEBT RT, the monolithic ferrite core (Case D) seems a reasonable choice which almost doubles the inductance factor of the HEBT prototype to a new value of A_L=2.6 µH. The dependency of maximum voltage and oscillation frequency on choice of capacitance C and winding number n is illustrated in the contour plots of Fig. 3. However, we stress that the HEBT prototype with a smaller inductance factor A_L=1.4 µH in principle meets all requirements. If a smaller capacitance value is to be used to boost the sensitivity S for measurements of smaller charges, Case D would produce the maximum sensitivity of S=200 µV at 30 kHz and 150 windings.

Let us assume that a segmented core has two air gaps. Then, for the same core cross section, the inductance factor drops from A_L=2.6 µH to 2.1 µH. To compensate

for this loss we need to increase cross section and volume (and possibly cost) by at least 20−25 %. Therefore, splitting the core does not offer any significant advantages.

A small reduction of 1 mm (12.9 instead of 13.0 cm) on the outer radius reduces the inductance factor by about 6 % to A_L=2.55 µH. A similar reduction is caused, if the inner radius is increased by 1 mm. A mechanical tolerance of the ferrite of ±1 mm in all three dimensions seems sufficient.

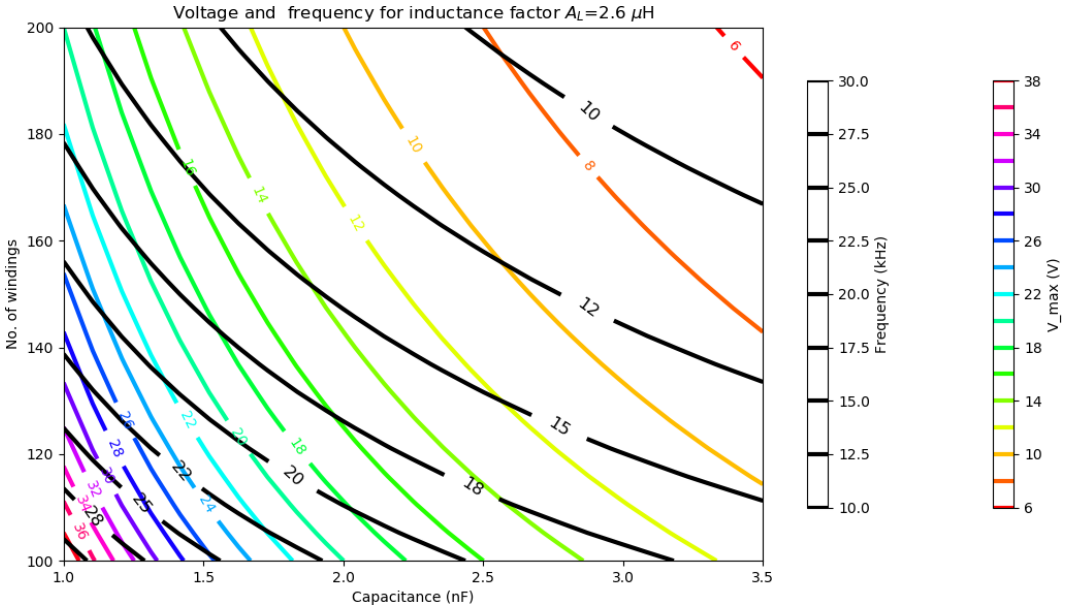

Figure 3: Contour plot of maximum voltage (colours) for the HEBT Case D (Q=4 µC) and oscillation frequency (black) for an assumed inductance factor A_L=2.6 µH. Contour lines of increasing sensitivity cross a fixed-frequency contour line at smaller capacitance values.

Table 4: Comparison of HEBT RT geometries with and without segmented ferrite core for resonance frequencies below 30 kHz. Maximum voltages were calculated for a number of 2.5x10^{13} protons.

Parameter		Case A	Case B	Case C	Case D
		segmented	segm.	segm.	monolithic Case A, no gaps
inner radius	r_i (cm)	11	12	11	11
outer radius	r_a (cm)	13	15	15	13
length (along beam)	h (cm)	4	3	4	4
cross section	A (cm^2)	2x4	3x3	4x4	2x4
volume estimate	V (cm^3)	600	765	1300	600
no. segments	N	2	2	2	0
total gap size	g (µm)	100	100	100	0
relative permeability	μ_r	2000	2000	2000	2000
effective permeability	μ_{eff}	1580	1618	1607	2000
inductance factor	A_L (µH)	2.1	2.2	4	2.6
Parameter set A					
capacitance	C (nF)	2.0	2.0	2.0	2.0
no. windings	n	100	100	100	100
frequency	ν (kHz)	24.6	24.0	17.8	22.1
sensitivity	S(10^8 e) (µV)	80	80	80	80
max. voltage (2.5x$10^{13}e$)	$V_C(max)$ (V)	13.3	13.3	13.3	13.3
Parameter set B					Set B / C
capacitance	C (nF)	0.5	1.0	1.0	1.0 / 0.5
no. windings	n	200	150	150	150 / 150
frequency	ν (kHz)	21.4	22.6	16.8	20.8 / 29.0
sensitivity	S(10^8 e) (µV)	160	106	107	106 / 212
max. voltage	$V_C(max)$ (V)	36.8	26.6	26.6	26.6 / 53.2

4.3 LA-RT for pBar Separator

Table 5 compares several choices for the pBar Separator. A minimum inductance factor A_L=2 µH is required to be able to achieve a sensitivity S close to 200 µV. Case A has a 50% larger core volume compared to Case D. For the latter case, the dependency of maximum voltage and oscillation frequency on choice of capcitance C and winding number n is illustrated in the contour plots Fig. 5.

Case E with slightly increased outer diameter has an inductance factor A_L=2.46 µH and a maximum sensitivity S=250 µV. This gives sufficient margin to guarantee a value above 2 µH in case 8 segments (instead of 6) are required (A_L=2.23 µH), the single gap size is 85 µm (instead of 50 µm) or the achieved relative permeability μ_r=1600 (instead of 2000). A sensitivity of S=200 µV is then still maintained, if one of the forementioned shortcomings occurs. A mechanical tolerance of the ferrite of ±1 mm changes the effective permeability by about 2.5 %.

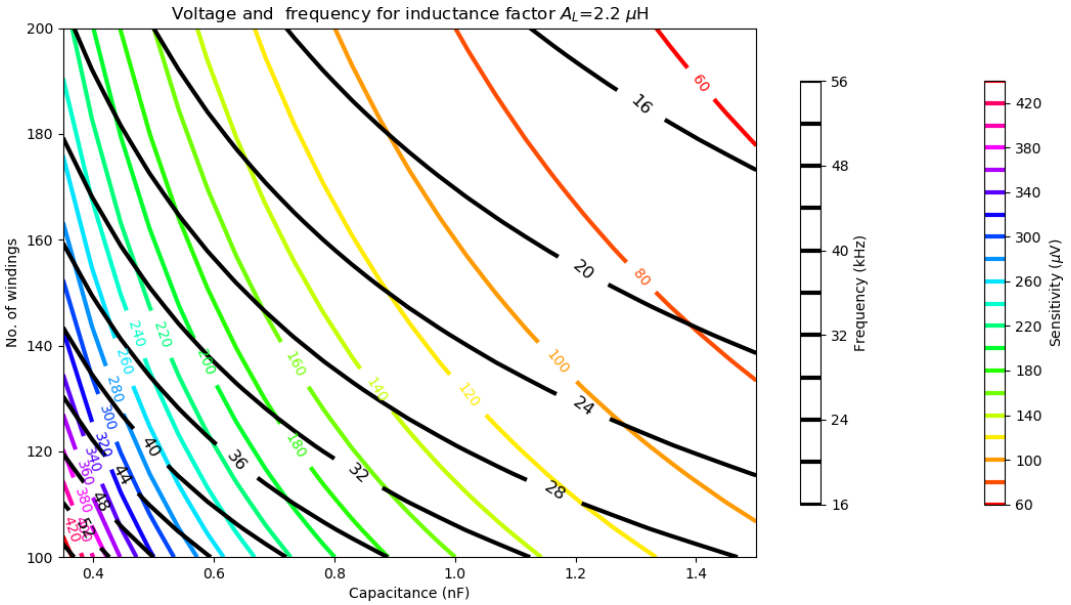

Figure 4: Contour plot of sensitivity S (colours) and oscillation frequency (black) for an assumed inductance factor A_L=2.2 µH (pBar Case D). Maximum voltages are 1000 times higher and range below 30 mV. Contour lines of increasing sensitivity cross a fixed-frequency contour line at smaller capacitance values.

Table 5: Main RT parameters for pBar Separator for resonance frequencies below 30 kHz. Maximum voltages were calculated for a number of 10^{10} pions.

Parameter		Case A	Case B	Case C	Case D	Case E
inner radius	r_i (cm)	21	21	21	21	21
outer radius	r_a (cm)	26	25	24.5	24.5	25
length (along beam)	h (cm)	5	4	4	5	5
cross section	A (cm^2)	5x5	4x4	3.5x4	3.5x5	4x5
volume estimate	V (cm^3)	3700	2310	2000	2500	2900
no. segments	N	8	8	6	6	6
total gap size	g (µm)	400	400	300	300	300
relative permeability	μ_r	2000	2000	2000	2000	2000
effective permeability	μ_{eff}	1297	1287	1409	1409	1413
inductance factor	A_L (µH)	2.77	1.8	1.74	2.17	2.46
Parameter set A						
capacitance	C (nF)	1.0	1.0	1.0	1.0	1.0
no. windings	n	150	150	150	150	150
frequency	ν (kHz)	20.2	25.0	25.4	22.8	21.4
sensitivity	S(10^8 e) (µV)	106	106	106	106	106
max. voltage	$V_C(max)$ (mV)	11	11	11	11	11
Parameter set B						
capacitance	C (nF)	0.5	0.5	0.5	0.5	0.35
no. windings	n	150	200	200	175	180
frequency	ν (kHz)	28.5	26.5	27.0	27.6	30.1
sensitivity	S(10^8 e) (µV)	212	159	159	182	253
max. voltage	$V_C(max)$ (mV)	21	16	16	18	25

5 Conclusions

Some critical issues concerning the reponse of RT detectors have been investigated. For the standard FAIR operation neither the longest bunches nor the longest batches seem to introduce integration errors beyond the 0.5% level. The effective quality factor of the ferrite material CMD 5005 at frequencies at 50 kHz is 22.5 and slowly increases towards the frequencies of interest below 30 kHz. Hence, the observation of a reasonable number of oscillation periods seems guaranteed.

Despite the production limits on the inner/outer dimensions, a monolithic core of 220/260 mm inner/outer diameter for the HEBT RT (Case D in Table 4) provides a larger inductance factor $L_0 \sim 2.6$ µH compared to the value of 1.4 µH of the HEBT prototype (see appendix B). Reasons are the reduction of the inner diameter and the length of 4 cm instead of 3 cm. A slightly higher sensitivity S= 80 µV (compared to S = 50 µV for the prototype) at an oscillation frequency of 22 kHz would produce maximum voltages below 50 V for 10 µC charge. We stress that this sensitivity can also be achieved with the HEBT prototype with n=100 at a frequency of 30 kHz. However, a sensitivity improvement using smaller capacitances would then result in oscillation frequencies around 40 kHz. For nominal pBar proton beams the maximum magnetic fields in the ferrite core is ∼2 mT, and the expected modification of the oscillation frequency due to changing permeability remains below a 5 % level.

For the LA-RT the hexagonal shapes (Cases D and E in Table 5) offer an inductance factor A_L >2 µH and seem to provide a good overall compromise. Since the maximum beam charge for the secondary beam lines is rather low, detector and electronics must be trimmed for high sensitivity S ∼200 µV. Core saturation or large capacitor voltages are of no concern. Integration error are negligible since only single bunches are detected.

Generally, the manufacturer must be asked to produce a ferrite material of maximum permeability. The aim is a smallest possible total air gap size and favours a hexagon over the octagon. Further, the measurement of the effective permeability is of great value for optimum choice of detector parameters.

In conclusion, ring core manufacturers should be asked for offers for the following geometries:

- HEBT: Case D
- pBar Separator: Case E

The ferrite production process must be tailored towards a high permeability value as the current estimates are based on a value μ_r=2000. But even, if the achieved permeability would be only μ_r=1600, the upper frequency limit of 30 kHz could be maintained with similar response for both types of transformers.

A Optimisation of inductance factor

If the cost of a ferrite core is linked to its volume V, we would like to achieve a large inductance factor A_L for a minimum volume. A simple-minded optimisation leads to the requirement of a small outer diameter.
Let us consider the ratio inductance factor/volume (A_L/V) for a toroid that we would like to assume a maximum value:

$$A_L = \mu_0 \cdot \mu_{eff} \left(\frac{h}{2\pi}\right) ln(r_a/r_i) \approx \mu_0 \cdot \mu_{eff} \left(\frac{A}{L}\right) \quad (18)$$

$$A = h \cdot (r_a - r_i) \quad (19)$$

$$L = \pi \cdot (r_a + r_i) \quad (20)$$

$$V = h \cdot \pi(r_a^2 - r_i^2) \quad (21)$$

$$A_L/V = \frac{\mu_0 \, \mu_{eff}}{L^2} \quad (22)$$

where A is the core cross section, L the mean magnetic length (mean circumference), and V the core volume. The ratio is independent of the length h, but depends strongly on the outer radius which defines the magnetic length L since the inner radius is typically well defined. Therefore, an increased length h should be preferred over a larger radius to increase the inductance.

B Comparison to other transformers

It may be instructive to compare the calculated sensitivities S with those of the existing GSI RT, the FAIR FCT (fast current transformer for current measurements), and the ICT (an integrating current transformer):

- HEBT prototype: The main parameters are C=2.15 nF, n=150, L_0=1.4 µH, and yield S∼50 µV (10^8 e). The CMD 5005 ferrite core has an inner/outer radius of 115/130 mm and a core cross section A=30x15 mm^2. The relative permeability of CMD 5005 is about 2000 (nominal). The stated value of L_0 indicates µ∼1900 and is in good agreement with the nominal value. The oscillation frequency is 19 kHz.

- Existing GSI RT: The main parameters are C=0.35 nF, n=100, L_0=8.6 µH, and yield S∼455 µV (10^8 e). This value is about a factor of 9 larger than that of the larger HEBT RT. The large inductance factor is due to the smaller radii of 81.5 mm (inner) and 102 mm (outer) and the high permeability of the Ferroxcube 3E25 material of 4000 (nominal). The stated inductance factor even indicates a value close to 5000. The core cross section is A=40x23 mm^2. The oscillation frequency is 29 kHz.

- FAIR FCT (S=0.5 V/A): A 50 ns pulse of 1x10^8 elementary charges generates an average signal of 160 µV which is comparable to the RT signal. Of course, this level drops for longer bunch lengths, and the broadband signal chain is more prone to spurious distortions and noise contributions. The calculated integral FCT charge value may suffer from these effects.
  FCTs with ten-fold higher sensitivity S=5 V/A (and even up to 10 V/A) are available, but produce very large peak voltages $V_C(peak)$ >500 V for short, intense proton bunches.

- Integrating Current Transformer (ICT): We refer to ICTs and their specifications as given by the manufacturer Bergoz. These devices are designed for very short bunches and respond with a Gaussian pulse shape of fixed length of 70 ns (standard) such that the integrated output voltage is proportional to the total passing bunch or batch charge. Hence, the sensitivity S is given in units of (Vs/As) and can reach values up to 20 (Vs/As). The intrinsic ICT's sensitivity is therefore similar to that of FCTs. As the shortest bunches of 50 ns length are about as long as the ICT response, high sensitivity ICTs would also generate rather large output voltages.
  As for the RT there are upper limits to the maximum length of a bunch of batch: for high sensitivity this limit drops to 100 ns, but for a sensitivity of 0.5 Vs/As (comparable to the FAIR FCT) this limit is 7.5 µs and above the longest batch times expected for FAIR operation. In this case, an ICT can be an alternative for absolute charge measurements.

C Parallel and series model

We establish the connection between parallel and series model, starting with equations (8) and (9) for the complex resistance, and equations (10) to (12) for the loss angle $tan(\delta_m)$ as given in reference [2].

$$Z_s = j\omega L_s + R_s \tag{23}$$

$$Z_p = \frac{1}{1/(j\omega L_p) + 1/R_p} \tag{24}$$

Further, we can make use of the definition of the loss angle $tan(\delta_m)$ given by the ratio of complex ($\mu^{''}$) and real ($\mu^{'}$) permeabilities:

$$tan(\delta_m) = \frac{R_s}{\omega L_s} = \frac{\mu_s^{''}}{\mu_s^{'}} \tag{25}$$

$$tan(\delta_m) = \frac{\omega L_p}{R_p} = \frac{\mu_p^{'}}{\mu_p^{''}} \tag{26}$$

$$\mu_p^{'} = \mu_s^{'} \cdot (1 + tan^2(\delta)) \tag{27}$$

$$\mu_p^{''} = \mu_s^{''} \cdot (1 + 1/tan^2(\delta)) \tag{28}$$

We rewrite the parallel resistance Z_p to obtain real and imaginary parts:

$$Z_p = \frac{1}{1/(j\omega L_p) + 1/R_p} = \frac{j\omega L_p R_p}{R_p + j\omega L_p} \tag{29}$$

$$= \frac{(j\omega L_p R_p)(R_p - j\omega L_p)}{(R_p + j\omega L_p)(R_p - j\omega L_p)} \tag{30}$$

$$= \frac{(\omega L_p)^2 R_p}{R_p^2 + (\omega L_p)^2} + j\omega \frac{L_p R_p^2}{R_p^2 + (\omega L_p)^2} \tag{31}$$

For a given frequency ω we can calculate the equivalent values for the series model:

$$R_s = \frac{(\omega L_p)^2 R_p}{R_p^2 + (\omega L_p)^2} = R_p \cdot \frac{1}{1 + Q^2} \tag{32}$$

$$L_s = \frac{\omega L_p R_p^2}{R_p^2 + (\omega L_p)^2} = L_p \cdot \frac{Q^2}{1 + Q^2} \tag{33}$$

where the relation $Q = \frac{\omega L_s}{R_s} = \frac{R_p}{\omega L_p}$ for the quality factor was used in the last step.

More generally, the transformation can be expressed for any frequency via the ratio of real to complex permeability:

$$R_s = \left(\frac{(\mu_p^{'}/\mu_p^{''})^2}{1 + (\mu_p^{'}/\mu_p^{''})^2} \right) R_p \tag{34}$$

$$L_s = \left(\frac{1}{1 + (\mu_p^{'}/\mu_p^{''})^2} \right) L_p \tag{35}$$

D Parameter plots for A_L=1.4 and 2.0 µH

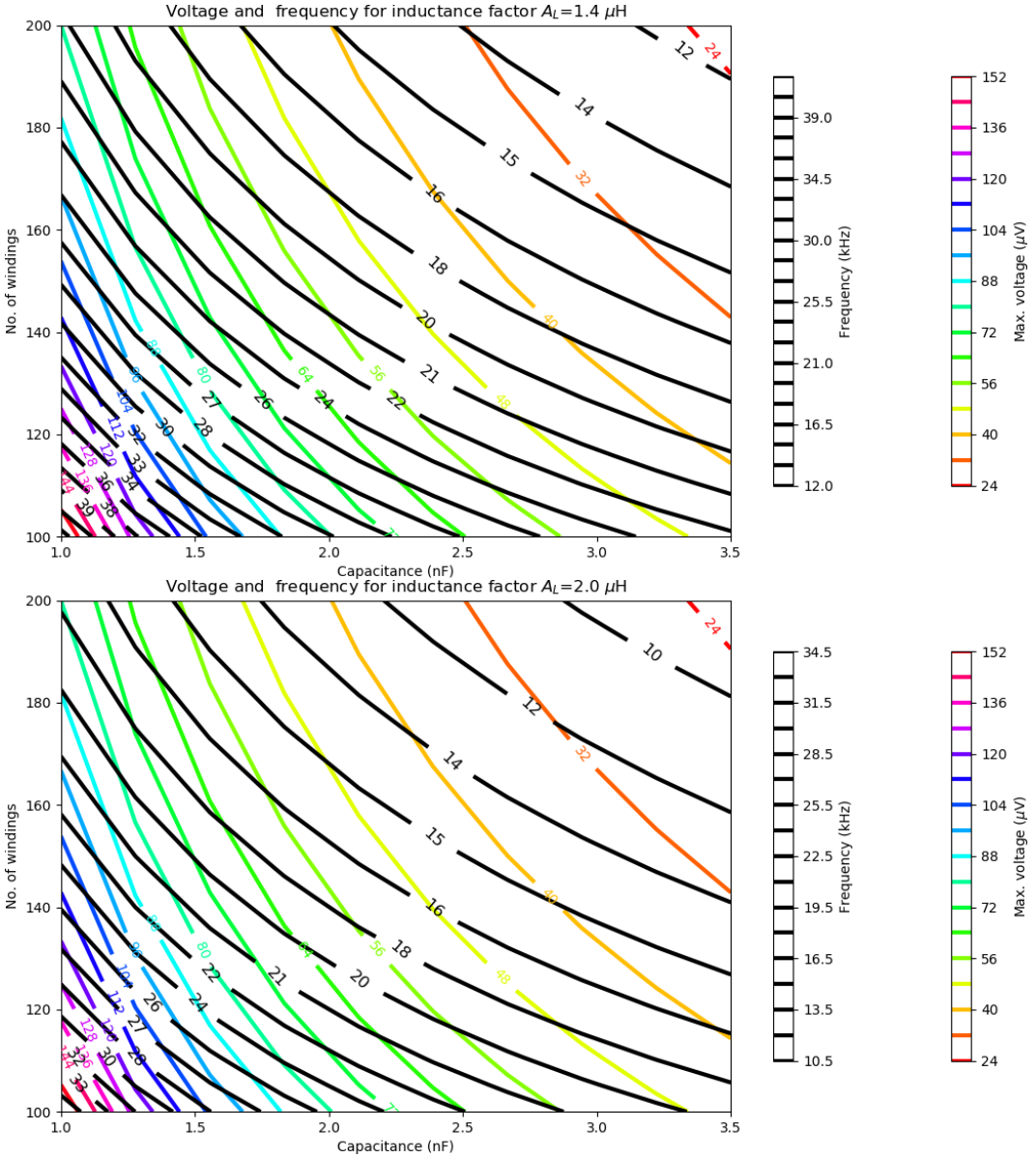

Figure 5: Contour plot of sensitivity S (colours) and oscillation frequency (black) for an assumed inductance factor A_L=1.4 (HEBT prototype) and 2.0 µH.

References

[1] TDR, "Ferrites and accessories - General Definitions", May 2017

[2] Ferroxcube, "Soft Ferrites and Accessories", Data Handbook, 2013

[3] P. Schütt, O. Geithner and P. Forck, "FAIR Operation Modes - Reference Modes for the Modularized Start Version (MSV)", April 2016

[4] Michael A. Clarke-Gayther, "A HIGH STABILITY INTENSITY MONITORING SYSTEM FOR THE ISIS EXTRACTED PROTON BEAM", TUPO79L, EPAC 1996

[5] R. Steiner, "Ein Induktionsmonitor zur Absolutmessung einzelner Strompulse nach dem Integrationsprinzip", Diplomarbeit, 1973, Institut für Kernphysik, Johannes Gutenberg-Universität Mainz

[6] National Magnetics Group, Inc., CMD 5005 data sheet, http://www.cmi-ferrite.com/Materials/Datasheets/NiZn/CMD5005.pdf